BIOCHEMICAL PHARMACOLOGY 72 (2006) 1646–1656

available at www.sciencedirect.com

ScienceDirect

journal homepage: www.elsevier.com/locate/biochempharm

Human equilibrative nucleoside transporter-1 (hENT1) is required for the transcriptomic response of the nucleoside-derived drug 5′-DFUR in breast cancer MCF7 cells

Míriam Molina-Arcas [a], *Gema Moreno-Bueno* [b], *Pedro Cano-Soldado* [a], *Héctor Hernández-Vargas* [b], *F. Javier Casado* [a], *José Palacios* [b,1], *Marçal Pastor-Anglada* [a,*]

[a] *Departament de Bioquímica i Biologia Molecular, Universitat de Barcelona, Diagonal 645, E-08028 Barcelona, Spain*
[b] *Programa de Patología Molecular, Centro Nacional de Investigaciones Oncológicas, Madrid, Spain*

ARTICLE INFO

Article history:
Received 14 July 2006
Accepted 31 July 2006

Keywords:
hENT1
5′-DFUR
Nucleoside transporter
cDNA microarray
Breast cancer

ABSTRACT

Nucleoside analogues are broadly used in cancer treatment. Although nucleoside metabolism is a necessary step in the development of their cytotoxicity, mediated transport across the plasma membrane might be needed for nucleoside-derived drugs to exert their pharmacological action. In this study, we have addressed the question of whether particular plasma membrane transporters contribute to the transcriptomic response associated with nucleoside-derived drug therapy. Firstly, we have characterized the nucleoside transporters responsible for 5′-DFUR uptake into the breast cancer cell line MCF7. 5′-DFUR is the immediate precursor of 5-FU and a metabolite of the orally administered pro-drug capecitabine, currently used in the treatment of breast cancer and other solid tumors. Although 5′-DFUR is a substrate for both plasma membrane equilibrative nucleoside carriers, hENT1 shows higher affinity for this molecule than hENT2. Inhibition of hENT1 function partially protected MCF7 cells from 5′-DFUR-induced cytotoxicity. Secondly, we have used a pharmacogenomic approach to determine how inhibition of hENT1 function contributes to the transcriptomic response associated to 5′-DFUR treatment. Under hENT1 inhibition most of the transcriptional targets of 5′-DFUR action, which were genes associated with apoptosis and cell cycle progression were blocked. This study demonstrates that although 5′-DFUR is substrate for both equilibrative nucleoside carriers, hENT1 function is essential for the full transcriptional response to 5′-DFUR treatment.

1. Introduction

Nucleoside analogs, such as capecitabine (5′-deoxy-5-fluoro-N-[(pentoxy)carbonyl]-cytidine; Xeloda®) and gemcitabine (2′,2′-difluoro-deoxycytidine; Gemzar®), and nucleobase derivatives, such as 5-fluorouracil (5-FU), are currently used in the treatment of breast cancer. Capecitabine is rapidly absorbed, metabolized in the liver by carboxylesterase to 5′-deoxy-5-fluorocytidine and then converted to 5′-deoxy-5-fluorouridine (5′-DFUR) by cytidine deaminase both in the liver and in tumor tissue. 5′-DFUR is the direct precursor of the cytotoxic drug 5-FU. This conversion occurs mostly in tumors, which express thymidine phosphorylase activity at different levels. Finally, 5-FU is converted to several active metabolites with effects at three different levels: inhibition of thymidylate synthase, disruption of RNA synthesis and DNA damage (see [1] for review).

Although nucleoside metabolism is a necessary step in the development of capecitabine cytotoxicity, mediated

* *Corresponding author*. Tel.: +34 93 4021543 (office)/4 (lab); fax: +34 93 4021559.
E-mail address: mpastor@ub.edu (M. Pastor-Anglada).
[1] Present address: Servicio de Anatomia Patológica, HHUU Virgen de Rocio, Sevilla, Spain.
0006-2952/$ – see front matter © 2006 Elsevier Inc. All rights reserved.
doi:10.1016/j.bcp.2006.07.036

transport across the plasma membrane is needed for nucleoside-derived drugs to exert their cytotoxic action. Two gene families are involved in the uptake of natural nucleosides and analogues: SLC28 (concentrative nucleoside transporters, CNT) and SLC29 (equilibrative nucleoside transporters, ENT) [2–4]. CNT proteins mediate high-affinity Na-dependent translocation of natural nucleosides and derivatives. In particular, hCNT1 is a high-affinity transporter for 5′-DFUR with a K_m around 200 μM [5]. hENT1 and hENT2 are broad-selectivity equilibrative carrier proteins, the former showing high sensitivity to pharmacological inhibition by the adenosine analogue nitrobenzylthioinosine (NBTI).

Nucleoside transport processes across the plasma membrane are not constitutive, nor is the pattern of isoform expression among different cell types and tissues [6]. Moreover, heterogeneity and selective loss of nucleoside transporter expression has been found in various tumors. In breast cancer, the analysis of a cohort of 33 patients showed variability of hENT1 expression among tumors, including four hENT1-negative cases [7]. Clinical correlations between equilibrative nucleoside transporters and tumor sensitivity to treatment have been reported. *Ex vivo* sensitivity to fludarabine of cells from chronic lymphocytic leukaemia (CLL) patients significantly correlates with hENT-mediated fludarabine transport and with hENT2 protein levels [8,9]. A significant correlation between hENT1 protein levels and survival was reported in a cohort of 21 patients suffering from pancreatic adenocarcinoma and treated with gemcitabine [10].

The particular ENT proteins implicated in 5′-DFUR uptake and cytotoxicity are not known, nor has the question of whether these plasma membrane proteins are required for its cytotoxic action been addressed. In this study we wanted, first, to identify the particular ENT proteins implicated in 5′-DFUR uptake and cytotoxicity, second, to determine whether the transcriptomic response to 5′-DFUR treatment could be elicited by short exposures to the drug, and third, to prove that NT-mediated uptake is actually responsible for the transcriptomic response to occur.

2. Materials and methods

2.1. Reagents

Uridine ([5,6-^{3}H], 35–50 Ci/mmol) was purchased from Amersham Biosciences (UK). 5′-DFUR ([6-^{3}H(N)], 3.2 Ci/mmol) and hypoxanthine ([2,8-^{3}H(N)], 40 Ci/mmol) were from Moravek Biochemicals (CA, USA). Uridine, hypoxanthine, 5′-DFUR, 5-fluorouracil, NBTI and dipyridamole were obtained from Sigma–Aldrich (Saint Louis, MO, USA).

2.2. Cell lines and culture conditions

Human breast carcinoma cell line MCF7 (HTB-22, ATCC-LGC Promochem Partnership, USA) was cultured in DMEM medium supplemented with 10% foetal bovine serum (GIBCO-BRL, Grand Island, NY), 2 mM glutamine and a mixture of antibiotics (100 U penicillin, 0.1 mg/ml streptomycin and 0.25 μg/ml fungizone). Cells were maintained as monolayer cultures at 37 °C in an atmosphere with 5% CO_2 and subcultured every 4–5 days.

2.3. Nucleoside uptake measurements in MCF7 cells

Nucleoside and nucleobase transport were measured by incubating cell monolayers in an uptake buffer (5.4 mM KCl, 1.8 mM $CaCl_2$, 1.2 mM $MgSO_4$ and 10 mM HEPES) supplemented with either 137 mM NaCl or 137 mM choline chloride, in which the labeled substrate was added at a final concentration of 1 μM (specific activity 1 μCi/nmol). When the desired incubation time had elapsed, transport was stopped by rapid aspiration of the uptake buffer followed by immediate washing in a cold stop solution, as previously described [11]. hENT1 activity was discriminated using NBTI 100 nM. hENT2-mediated transport was measured using hypoxanthine 1 μM in sodium-free medium both in the presence and in the absence of dipyridamole 10 μM.

2.4. Cytotoxicity assays

The cytotoxicity assays were performed by seeding MCF7 cells at a density of 20,000 cells/cm^2 in 24-well culture plates. Twenty-four hours after seeding, cultures were exposed for 90 min to increasing concentrations of 5′-DFUR or 5FU (from 10 μM to 3 mM), either in presence or absence of NBTI 100 nM. NBTI was pre-incubated 15 min before drug addition. Viability was assessed 48 h after the addition of the cytotoxic drugs by counting the cells in the monolayer after trypsinization of the cultures (Multisizer; Beckman Coulter, Inc., Fullerton, CA). Data were fitted to a concentration response curve, using GraphPad Prism 4.0 software (GraphPad Sofware, Inc., San Diego, CA) to obtain the IC_{50}.

2.5. Cell cycle analysis

Cells were seeded at 20,000 cells/cm^2 in six-well culture plates and treated with 5′-DFUR. After treatment, cells were harvested, fixed with 70% ethanol (v/v) and stored for 24 h at 4 °C. After centrifugation at 1200 rpm for 4 min cells were resuspended in phosphate buffered saline (PBS) containing 10 μg/ml RNAse and their DNA content was measured after propidium iodide staining (100 μg/ml). Fluorescence-activated cell-sorting analysis was carried out using a FACScan flow cytometer (Becton Dickinson, Franklin Lakes, NJ).

2.6. RNA isolation and T7 amplified RNA preparations

MCF7 cells were seeded in 75 cm^2 flasks at a density of 20,000 cells/cm^2. After 24 h cells were treated for 90 min with 5′-DFUR 250 μM either in the presence or in the absence of NBTI 100 nM. NBTI was pre-incubated 15 min before 5′-DFUR addition. 4 and 24 h after the beginning of the 90 min-treatment cells were trypsinized and total RNA was isolated using Rneasy Mini Kit (Qiagen, Hilden, Germany). The quality of the RNA was measured spectrophotometrically by the A260/A280 absorbance ratio. T7-amplified RNA was synthesized as described elsewhere [12]. Briefly, 3 μg of total RNA and oligo-dT primer containing a T7 RNA polymerase promoter was used

Table 1 – Primers used for semiquantitative RT-PCR analysis

Gene	Accession no.	Primer sequence (5′–3′)	Product size (pb)	Number cycles
GAPDH	NM002046	Fw: TGGTATCGTGGAAGGACTCATGAC; Rv: ATGCCAGT-GAGCTTCCCGTTCAGC	188	22
TP53I3	NM004881	Fw: GTGCACTTTGACAAGCCGGGAGGA; Rv: CAGCCTGGGT-CAGGGTCAATCCCT	346	35
FDXR	NM004110	Fw: GGAAATTCCTGGTGAGGAGC; Rw: CTGGAGACCCAAGAAATCCAC	385	33
PPM1D	NM003620	Fw: GAGCACTTGTGGGGTTTCATC; Rw: CCACCAAGTCCTTCGATTCG	347	30
TP53INP1	NM033285	Fw: CCATGCAAACTGTTCCTGTT; Rw: TCTCCCAGTACAAGGAGCAG	403	40
GADD45A	NM001924	Fw: GGAGGAAGTGCTCAGCAAAG; Rw: GCAGGATCCTCCCATTGAGA	348	40

to amplify the double strand cDNA synthesis with Superscript Choice System (Life Technologies, Inc., Gaithersburg, MD). *In vitro* transcription was conducted with the Megascript T7 kit (Ambion, Austin, TX). Amplified RNA (aRNA) was purified using TRIZOL and the integrity was measured spectrophotometrically and by gel electrophoresis.

2.7. Labeling and hybridizations

A 3 μg of the test or reference amplified RNA was labelled with fluorescent Cy5 and Cy3, as described [12]. In all microarray experiments, each sample was co-hybridized with a pool of amplified RNAs obtained from the Universal Human RNA (Stratagene, La Jolla, CA), used as a reference. To ensure the reproducibility of the technique cDNA hybridization was performed in duplicate in all cases, using reciprocal labelling. Moreover, RNA from two independent experiments was isolated. Thus, four microarrays were hybridized for each condition. Hybridization was performed in 4× standard sodium citrate, 1× bovine serum albumin, 2 μg/ml DNAs and 0.1% sodium dodecyl sulfate at 42 °C for 15 h. Slides were washed, dried and then scanned in a Scanarray 5000 XL (GSI Lumonics, Kanata, Ont., Canada) and images were analysed using the GenePix 4.0 program (Axon Instruments Inc., Union City, CA). All the microarray raw data tables have been deposited in the Gene Expression Omnibus under the accession number of GSE2930 and GSE2931 (submitter M. Molina-Arcas).

The cDNA array chip is a new version of the Spanish National Cancer Center (CNIO) Oncochip (v2.0). This version contains 11,500 cDNA clones corresponding to 9300 different genes (http://bioinfo.cnio.es/data/oncochip). Most of the clones have been printed in duplicate to assess reproducibility.

2.8. Data analysis

To adjust differences in the labelling, Cy5/Cy3 ratios were normalized with the Diagnosis and Normalization of Microarray Data (DNMAD), tool based on standard print-tip losses [13]. Before normalization, bad spots or areas showing defects were flagged by hand.

To organize patterns on a symmetrical scale, ratios were log-transformed (base 2), duplicate spots were averaged to the median and missing data were filtered. Data were preprocessed as described [14]. To obtain the expression profile, medians of ratios of each point were calculated and each condition was referred to its control. All genes which showed variability bigger than 10% of the S.D. in one condition were not further considered. For statistical analysis, we selected genes whose expression differed by at least 75% (0.8-fold) from the respective control.

2.9. Semi-quantitative and quantitative RT-PCR

Semi-quantitative and quantitative RT-PCR were performed to validate data of cDNA microarrays of selected genes. One microgram of total cellular RNA was used to generate cDNA, using Superscript II system and random primers for reverse transcription (Life Technologies).

For semi-quantitative RT-PCR of selected genes, primer sequences, annealing temperature and number of cycles are listed in Table 1. After establish correct cycling parameters to allow measurements in the exponential phase, semi-quantitative RT-PCR was performed by denaturation for 5 min at 95 °C, followed by 22–40 cycles of PCR amplification: 94 °C denaturing for 5 s, 55 °C annealing for 30 s, and 72 °C extension for 30 s, and a final extension of 5 min at 72 °C. Densitometric analysis was done using Phoretix 1D Software. Semiquantitative analysis was carried out by calculating the densitometry ratios versus GAPDH.

Quantitative real-time PCR was performed with the ABI PRISM 7700 Sequence Detection System (Applied Biosystems, Foster City, CA), using the manufacturer's recommended conditions. Assays-on-Demand Taqman probes (Applied Biosystems) of CDKN1A/p21, TNFRSF6/FAS, AQP3, RRM2B, RPL3 and GAPDH were used. Relative quantification of gene expression was performed as described in the TaqMan user's manual using GAPDH as internal control.

2.10. Immunoblotting and immunocytochemistry

Control and treated cells were lysed in RIPA buffer containing a protease inhibitor cocktail (Complete MINI, Roche). A 5–40 μg of each protein extract was separated on 10–12% polyacrylamide gels and transferred to Immobilon-P (Millipore, Bedford, MA) membranes. Following antibody incubation with monoclonal anti-p53 DO7 (Novocastra, Newcastle, UK) and anti-Bcl-2 (Santa Cruz Biotechnology, CA) and polyclonal anti-Bax (Santa Cruz Biotechnology, CA) proteins were detected using secondary antibodies conjugated to horseradish peroxidase and an enhanced chemiluminescence (ECL) detection kit (Amersham, Buckinghamshire, UK). Protein loading was confirmed with α-tubulin (Oncogene Research, Boston, MA). Densitometric analysis was done

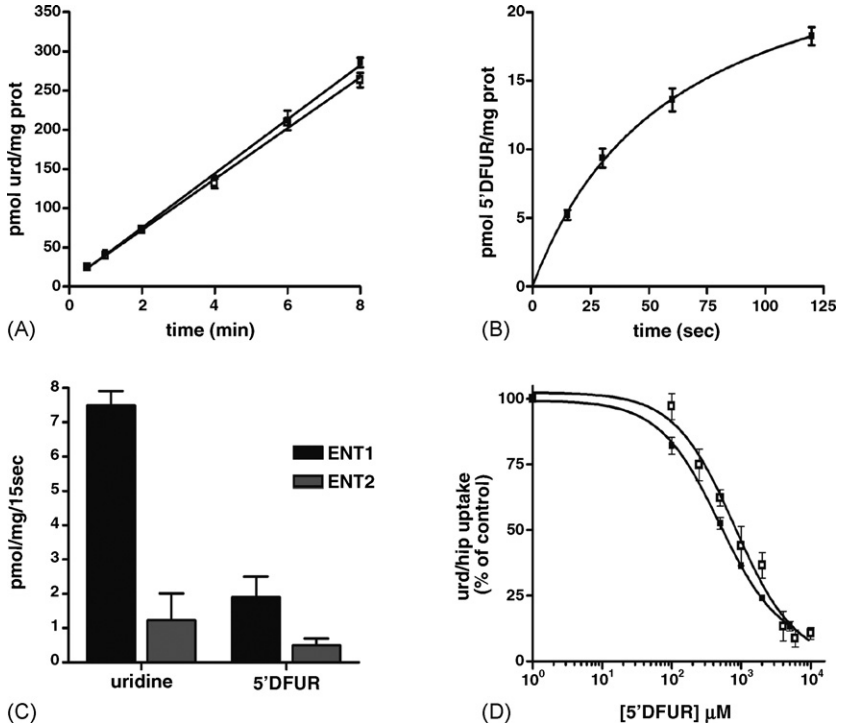

Fig. 1 – Characterization of nucleoside transport into MCF7 cells. (A) Time course of uridine uptake by MCF7 cells. Cells were incubated with 1 μM uridine either in NaCl (■) or choline chloride medium (□). (B) Time-course of 5′-DFUR uptake. Cells were incubated at different times (15–120 s) with 1 μM 5′-DFUR in choline chloride medium. (C) Discrimination of equilibrative uridine and 5′-DFUR uptake. A 1 μM uridine and 1 μM 5′-DFUR transport was measured under initial velocity conditions (15 s). To determine the contribution of equilibrative transport activity, 100 nM NBTI inhibition was used to discriminate between NBTI-sensitive (ENT1) and NBTI-insensitive transport rates. (D) 5′-DFUR inhibition of hENT1 (■) and hENT2 (□). hENT1-dependent uptake was calculated by subtracting the 100 nM NBTI-insensitive uridine uptake from the uridine uptake in choline chloride medium. hENT2-dependent transport was measured by subtracting the 10 μM dipyridamole-insensitive hypoxanthine uptake from the hypoxanthine transport in choline chloride medium. Cells were incubated with 1 μM uridine or hypoxanthine for 1 min in the presence of increasing concentrations of 5′-DFUR. Results are shown as percentage of control values (absence of inhibitor). Results are the mean ± S.E. of three to five independent experiments measured in quadruplicate.

using Phoretix 1D Software. Semiquantitative analysis was carried out by calculating the densitometry ratios versus α-tubulin.

To check the expression and localization of Mdm2, cells were seeded at a concentration of 20,000 cells/cm^2 on glass coverslips and placed in 24-well plates. After treatment cells were washed in PBS, fixed with 2% paraformaldehyde–0.06 M sucrose in PBS for 15 min and permeabilized with 1% Triton X-100 in PBS. Cells were subsequently washed in PBS and treated with blocking solution (1% BSA in PBS) for 15 min. Incubation with primary monoclonal antibody against Mdm2 (Santa Cruz Biotechnology, CA) was performed for 1 h at room temperature. Cells were washed in washing buffer (0.1% Triton X-100, BSA 0.1% in PBS) and incubated with secondary antibody (anti-mouse antibody conjugated to Alexa-568, Molecular Probes) for 45 min at room temperature in the dark. Coverslips were rinsed once for 10 min with washing buffer and twice with PBS and finally mounted with medium suitable for immunofluorescence (Mowiol, Calbiochem, San Diego, CA). Samples were analyzed using confocal microscopy (Olympus Fluoview).

2.11. *Statistical analysis*

The unpaired Student's *t*-test was used to compare experimental data. This analysis has been carried out using GraphPad Prism software (GraphPad Software, Inc., San Diego, CA)

3. Results

3.1. *Characterization of nucleoside transport into MCF7 cells*

A basal characterization of the transport processes involved in nucleoside uptake into the model cell line MCF7 was performed. Uridine was initially used as substrate because it is recognized by all cloned plasma membrane nucleoside transporters. A 1 μM uridine uptake was monitored in MCF7 cells either in the presence or the absence of sodium. Uridine uptake was linear for 8 min and it was exclusively mediated by equilibrative nucleoside transporters (Fig. 1A). The time-courses of cytidine and guanosine uptake were lineal for

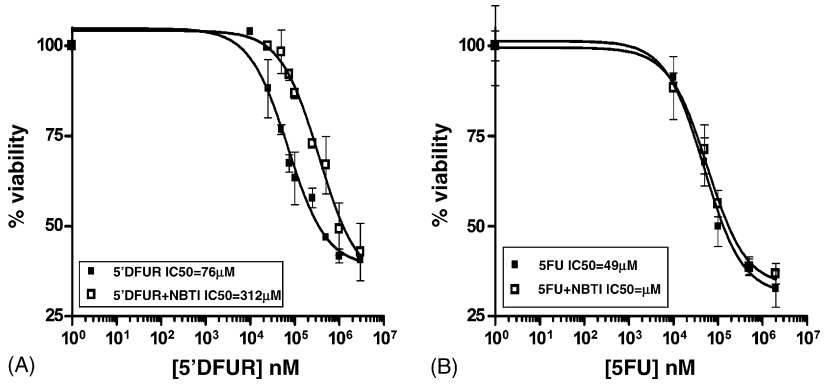

Fig. 2 – Cytotoxicity of 5′-DFUR and 5FU in MCF7 cells. Cell viability was assessed by cell counting (Multisizer) 48 h after 90 min exposure to 5′-DFUR (A) or 5FU (B). After 24 h seeding cells were treated for 90 min with increasing concentrations of the drug in the absence (■) or the presence of NBTI (□) 100 nM. Viability was calculated on a percentage basis by comparing the number of cells after treatment with that of a culture that had not been exposed to the drug. Results are the mean ± S.E. of three independent experiments measured in quadruplicate.

several minutes and did not show any Na-dependent uptake (data not shown). Although nucleoside uptake was only mediated by equilibrative transporters, real-time RT-PCR from MCF7 cells revealed that the three SLC28 genes (encoding CNT1, CNT2 and CNT3 proteins) transcribed their corresponding mRNAs (not shown).

To determine the major routes involved in 5′-DFUR transport in MCF7 cells, we monitored the uptake of 1 μM [^{3}H]-5′-DFUR. Linear velocity conditions were lost before the first minute of incubation (Fig. 1B). As for uridine, 5′-DFUR transport was mediated exclusively by equilibrative nucleoside transporter. In order to discriminate between NBTI-sensitive and -insensitive components of nucleoside transport (hENT1 and hENT2-mediated, respectively), 1 μM [^{3}H]-uridine and [^{3}H]-5′-DFUR uptake were monitored either in the presence or in the absence of 100 nM NBTI. Transport was measured at 15 s (Fig. 1C). Uridine uptake was four-fold higher than 5′-DFUR, but for both substrates transport was mostly NBTI sensitive, and thus associated with hENT1.

The interaction between 5′-DFUR and hENT1 and hENT2 transporters was then assessed in MCF7 cells by monitoring the inhibition of 1 μM uridine and hypoxanthine uptake, respectively, triggered by different concentrations of 5′-DFUR (Fig. 1D). IC_{50} values of 5′-DFUR inhibition of hENT1 and hENT2 were 489 ± 22 and 1027 ± 288 μM, respectively. The substrates used to obtain 5′-DFUR IC_{50} were different. Thus, to compare the 5′-DFUR affinity to hENT1 and hENT2 transporters we calculate the K_i values using the Cheng-Prusoff equation [15]. The K_i values (486 μM for hENT1 and 1020 μM for hENT2) indicated that hENT1 recognized 5′-DFUR with higher affinity than hENT2.

3.2. 5′-DFUR and 5FU cytotoxicity

5′-DFUR cytotoxicity was measured at 48 h after a 90 min-treatment with increased concentrations of the drug (Fig. 2A). To assess the putative role of the hENT1 transporter in 5′-DFUR sensitivity, the hENT1-related transport activity was inhibited by 100 nM NBTI. The inhibition of hENT1 activity produced a four-fold increase in the IC_{50} (76 ± 1.3 and 312 ± 12 μM, respectively) (Fig. 2A) and also increased the IC_{50} after a 24 h-treatment (16 and 78 μM, respectively) (data not shown). Moreover, inhibition of both equilibrative nucleoside transporters with dipyridamole induced a significant resistance (IC_{50} > 3 mM) to 5′-DFUR (data not shown).

To determine whether hENT1-mediated sensitivity was specific for hENT1 substrates, 5FU cytotoxicity was measured either in the presence or in the absence of NBTI 100 nM (Fig. 2B). 5FU sensitivity was independent of the inhibition of hENT1, and the IC_{50} values (49 and 58 μM, respectively) were similar to those recorded for 5′-DFUR.

To examine the growth-inhibitory effects of 5′-DFUR we analyzed the cell cycle events at the same moment that the RNA extraction for microarray experiments was made. At 4 h there was in a slight increase in the number of cells in G1-phase (Fig. 3). This effect was not blocked by NBTI. At 24 h cells accumulated in S-phase, consequent to an inhibition of DNA synthesis. When hENT1 activity was inhibited by NBTI the effect on the cell cycle was similar to control (Fig. 3).

3.3. Gene expression profiles after 5′-DFUR treatment in MCF7 cells

To determine the role of equilibrative nucleoside transporter in the action of 5′-DFUR we monitored the gene expression profile of MCF7 cells after 90 min treatment with 5′-DFUR 250 μM, either in presence or in the absence of NBTI, at 4 and 24 h, using the CNIO Oncochip. RNA from two independent experiments was isolated, labeled and hybridized as described in Section 2. Initial exploration of the dataset using the Preprocessor tool [14] revealed that 5′-DFUR did not alter the expression of most of the genes on the Oncochip. Forty genes were upregulated by at least 75% and 28% were down-regulated. Most of the changes in gene expression were obtained at 24 h, whereas, few changes were evident at 4 h.

Table 2 lists some of the genes showing altered expression 24 h after 5′-DFUR treatment. Most of them were up-regulated and their increase was either partially or totally blocked when

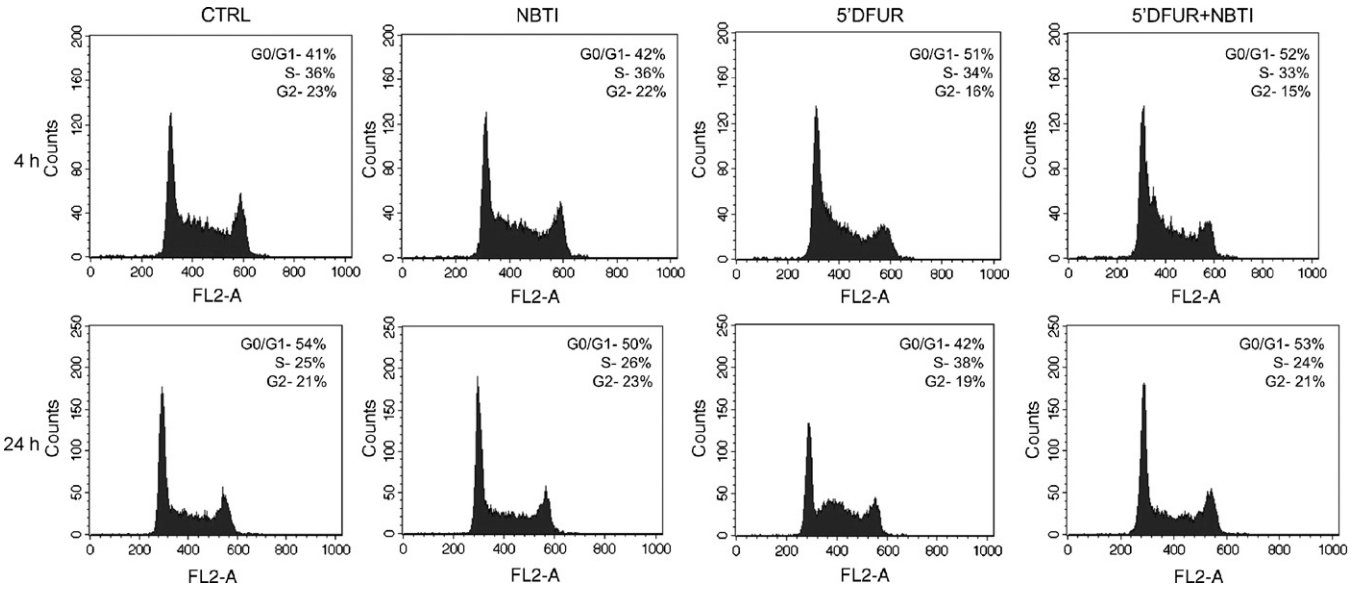

Fig. 3 – Effect of 5′-DFUR on cell cycle. Cells were treated for 90 min with 5′-DFUR either in presence or in the absence of NBTI 100 nM. 4 and 24 h after the beginning of the 90 min-treatment DNA content was measured on asynchronously growing cells using propidium iodide staining and fluorescence-activated cell sorter analysis. Results are representative of those obtained in three independent experiments.

hENT1 activity was inhibited (Table 2). Moreover, 12 genes are p53 targets, including *CDKN1A/p21*, *TNFRF6/FAS*, *MDM2*, *RRM2B* (ribonucleotide reductase M2B) and *PPM1D* (protein phosphatase 1D magnesium-dependent).

3.4. *Validation of microarray results*

To confirm the differential expression observed by cDNA microarray analysis, validation using semiquantitative and

Table 2 – Functional grouping of genes identified by cDNA microarray analysis as being regulated by 5′-DFUR in MCF7 cells

Gene symbol[c]	Fold change[a]			% inhibition[b]	Gene
	NBTI	5′-DFUR	5′-DFUR + NBTI		
Ribosomal proteins					
RPL3	0.03	−1.02	−0.70	25	Ribosomal protein L3
RPL10A	0.10	−0.82	−0.75	5	Ribosomal protein L10a
SNRPG	−0.10	−0.81	−0.25	47	Small nuclear ribonucleoprotein polypeptide G
RPS27L	0.25	1.26	0.50	59	Ribosomal protein S27-like
Cell cycle					
CCNG1	−0.12	1.15	0.39	75	Cyclin G1
SESN1	−0.03	1.29	0.42	77	Sestrin 1
CDKN1A	0.07	2.54	0.69	87	Cyclin-dependent kinase inhibitor 1A (p21, Cip1)
p53 regulation					
PPM1D	−0.31	0.92	0.28	76	Protein phosphatase 1D magnesium-dependent
MDM2	0.04	1.18	0.30	82	Mdm2,p53 binding protein (mouse)
Apoptosis					
TP53I3	0.02	0.80	0.23	77	Tumor protein p53 inducible protein 3
BAX	0.18	0.83	0.49	48	BCL2-associated X protein
TNFRSF6	−0.04	2.28	0.83	80	Tumor necrosis factor receptor superfamily, member 6
TP53INP1	−0.29	2.56	0.77	86	Tumor protein p53 inducible nuclear protein 1
Other					
RRM2B	−0.21	0.87	0.16	86	Ribonucleotide reductase M2 B (TP53 inducible)
FDXR	0.03	0.90	0.53	49	Ferredoxin reductase
AQP3	0.04	1.23	0.29	83	Aquaporin 3

[a] Fold change (log 2) referred to 24 h-control after a treatment of 90 min with 5′-DFUR 250 μM.
[b] Percentage of inhibition of 5′-DFUR + NBTI vs. 5′-DFUR.
[c] p53 related genes are written in bold letters.

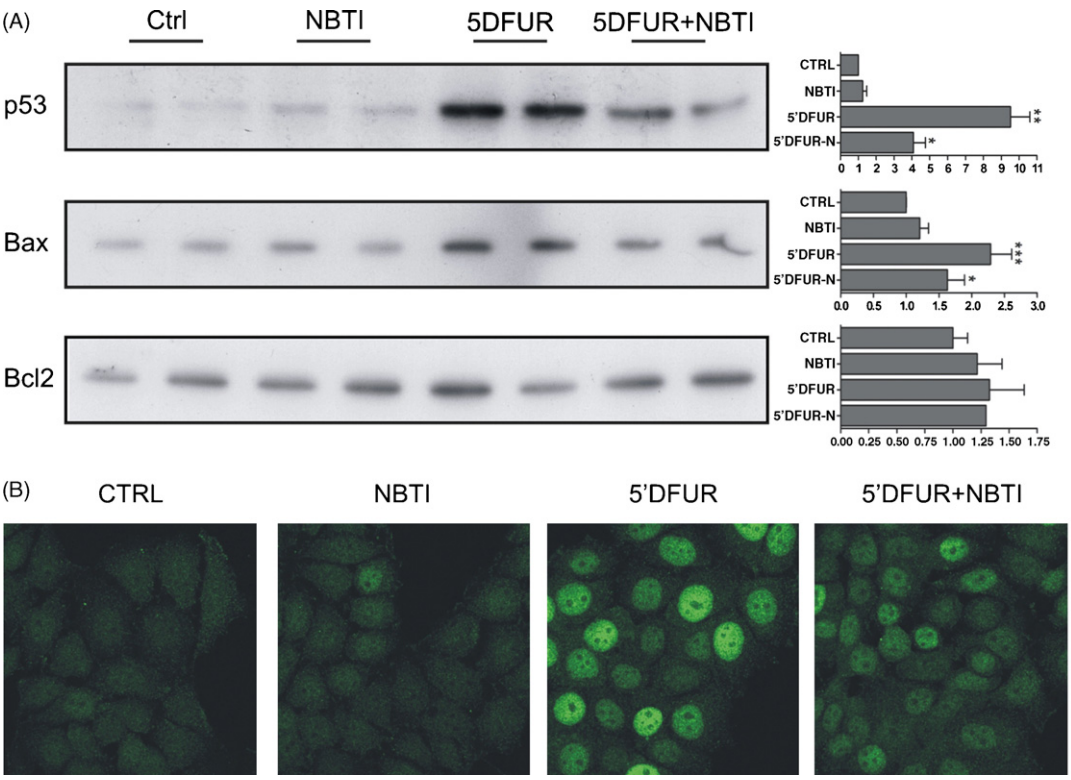

Fig. 4 – Validation of microarray results. (A) Western blot analysis of p53, Bax and Bcl2 protein expression 24 h after a 90 min treatment with 5′-DFUR 250 μM. The induction triggered by treatment was quantified densitometrically. Results (mean ± S.E.M. of three to five independent experiments) are shown as arbitrary units normalized to α-tubulin and control (non-treated cells). A representative western blot is shown. Statistical significance was assessed using the Student's t-test ($^{*}P < 0.05$, $^{**}P < 0.01$, $^{***}P < 0.001$). (B) Immunocytochemistry of Mdm2 in MCF7 cells. Cells were treated 90 min with 250 μM 5′-DFUR in presence or absence of NBTI 100 nM. At 24 h expression and localization of Mdm2 were analyzed as described in Section 2.

quantitative techniques was performed for a group of selected genes involved in apoptosis and cell cycle.

p53 protein was up-regulated nearly 10-fold at 24 h although *p53* transcripts were unchanged (Fig. 4A). This increase was also detected at 4 h (data not shown). Protein levels of Bax were also induced in response to 5′-DFUR, whereas Bcl-2, which was not differentially expressed in microarray analysis, was unchanged (Fig. 4A). Fig. 4B shows nuclear immunocytochemical localization of Mdm2 protein following 5′-DFUR treatment, which is consistent with *MDM2* up-regulation recorded in microarray experiments.

A series of genes (*TP53I3*, *PPM1D*, *FDXR* and *TP53INP1*) was validated using semiquantitative RT-PCR (Fig. 5). Up-regulation after 5′-DFUR treatment was confirmed. Moreover, for all checked genes, but *FDXR*, we were able to confirm a 75–80% inhibition of gene induction when NBTI was added. To demonstrate that the cutoff of 0.8 was suitable for the transcriptomic approach, we also confirmed the up-regulation of *GADD45A*, which was induced by 50% in our microarray experiments (Fig. 5).

mRNA expression of *CDKN1A/p21*, *TNFRF6/FAS*, *RRM2B*, *AQP3* and *RPL3* were examined using quantitative real-time PCR (Fig. 6). Gene up-regulation induced by 5′-DFUR was partially blocked when NBTI was added, whereas decrease of *RPL3* expression was not inhibited by NBTI. Moreover, a weaker induction of *CDKN1A/p21* and *TNFRF6/FAS* was detected at 4 h (data not shown). To demonstrate the relevance of a transient treatment in the long-term response to 5′-DFUR, the effect of a continuous (24 h) exposure to the drug on the transcriptomic response of selected genes was also analyzed (Fig. 6). Under these conditions no significant differences with the 90 min treatment data were observed.

4. Discussion

The nucleoside analogue 5′-DFUR is the immediate precursor of 5-FU and a metabolite of the orally administered pro-drug capecitabine, broadly used in the treatment of breast cancer and other solid tumors. We had previously reported that hCNT1 is a high-affinity transporter for 5′-DFUR, with a K_m around 200 μM, and that heterologous expression of hCNT1 increases sensitivity to the drug [5]. However, hCNT1 protein expression is lost in some tumors more frequently than hENT1 and hENT2 [16]. In this study, we have studied the role of equilibrative nucleoside transporters in 5′-DFUR bioavailability in breast cancer cells by analyzing the effect of inhibition of

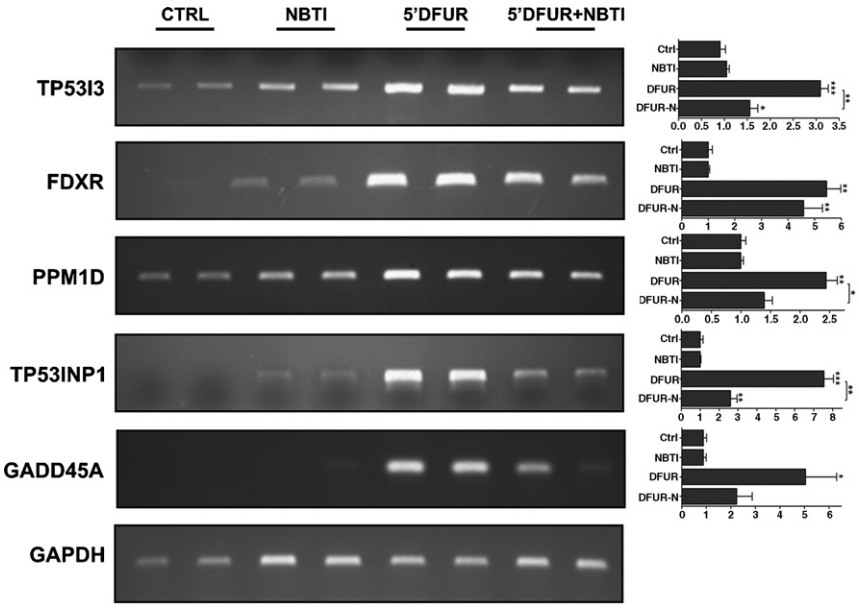

Fig. 5 – Semi-quantitative RT-PCR analysis for TP53I3, FDXR, PPM1D, TP53INP1 and GADD45A, 24 h after 90 min-treatment with 5′-DFUR. GAPDH was used as internal control. Samples were analyzed as described in Section 2. The magnitude of the induction triggered by treatment was quantified densitometrically. Results (mean ± S.E.M. of three to five independent experiments) are shown as arbitrary units normalized to GAPDH and control (non-treated cells). A representative PCR for each gene is shown. Statistical significance was assessed using the Student's *t*-test ($^{*}P < 0.05$, $^{**}P < 0.01$, $^{***}P < 0.001$).

hENT1 by NBTI on drug sensitivity and the associated transcriptomic response.

We have demonstrated that 5′-DFUR is a substrate for the equilibrative nucleoside carriers, but hENT1 shows higher affinity than hENT2. Inhibition of hENT1 by NBTI partially protected MCF7 cells from 5′-DFUR-induced cytotoxicity, resulting in a four-fold increase in the IC_{50}. NBTI also afforded protection from 5′-DFUR in MDA-MB-435s cells [7] and from gemcitabine in a panel of cell lines [17]. Indeed, in a variety of cell types, hENT1 deficiency has been associated with nucleoside drug resistance [18]. Accordingly, the induction of resistance by NBTI was specific for hENT1-substrates, and so 5-FU cytotoxicity was not affected by its inhibition. 5′-DFUR also induced cells to accumulate in S-phase, as previously shown for 5-FU [19]. In contrast, NBTI addition reverted the 5′-DFUR effect and restored the cell cycle distribution profile. Interestingly, although the dose used was close to the IC_{50} for 5′-DFUR + NBTI most of the transcriptional changes produced by this drug were blocked. In fact, microarrays data as well as validation of these results using other techniques demonstrated that NBTI blocked in a 75–85% the transcriptional response to 5′-DFUR. Thus, our results suggest that, at least in cells with no active hCNT1 present, hENT1 is necessary for 5′-DFUR-mediated cytotoxicity and its deficiency may contribute to capecitabine resistance.

In this study we have used a pharmacogenomic approach to analyze the role of hENT1 in the drug-mediated responses during cancer treatment and to identify genes regulated by 5′-DFUR. The most innovative aspect of our approach consists in a brief 90 min exposure of MCF7 cells to 5′-DFUR and then an analysis 4 and 24 h later, instead of the longer, several-day treatments of previous reports [20,21]. In fact, our schedule is closer to that found *in vivo*, since, 5′-DFUR plasma concentrations peak 1 h after oral administration of capecitabine (825 mg/m^2), and it is no longer detected 3 h after intake [22]. Moreover, these conditions allow a better evaluation of the particular role nucleoside transporters might play in chemosensitivity.

The present approach has identified 68 genes, out of 9300 analysed, as transcriptionally regulated in response to 5′-DFUR treatment. These results are somehow consistent with previous studies in which other nucleoside-related drugs, but not 5′-DFUR were used. Troester et al. analyzed a cohort of breast cancer tumors before and after treatment with 5-FU and found 23 genes with increased expression in the after-samples [20]. Using gene expression profiling only 27 genes were transcriptionally modified in CLL patients after fludarabine treatment [23]. Therefore, our results suggest that short term exposures are enough to achieve a complete transcriptional response, and that the number of induced genes are similar to those obtained *in vivo*.

Activation, rather than repression, appears to be the most common response of 5′-DFUR-regulated genes. Among these, 12 have been identified as p53 targets in a variety of systems, involved in apoptosis (*TP53I3/PIG3*, *TNFRSF6/FAS*, *P53INP1*), growth arrest (*CDKN1A/p21*) and xenobiotic metabolism (FDXR) [24–26]. To confirm the activation of this pathway, p53 protein and *CDKN1A/p21* mRNA were shown to be up-regulated 4 h after 5-DFUR treatment. Although changes in gene expression caused by 5′-DFUR were similar to those described previously for 5-FU in different studies using cDNA microarrays [20,27,28], three new genes have been identified

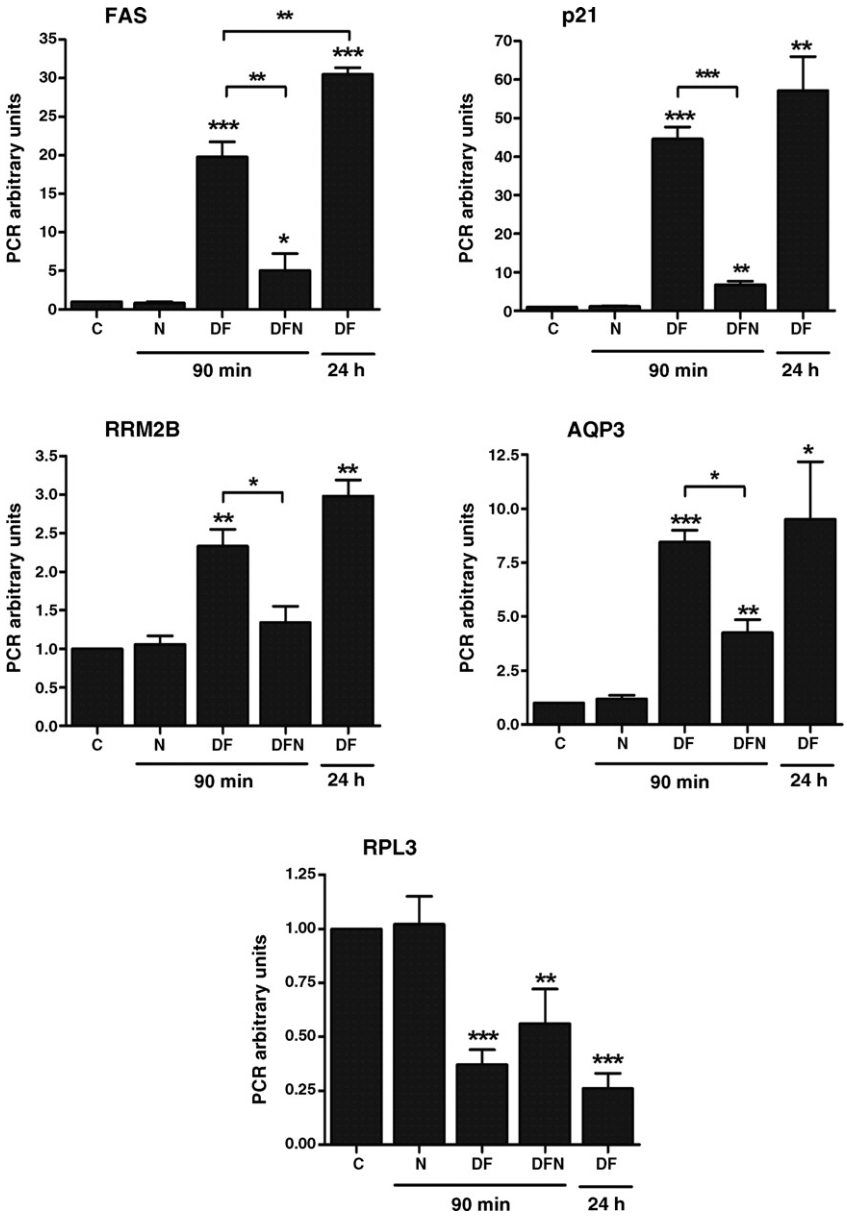

Fig. 6 – Quantitative RT-PCR analysis for CDKN1A/p21, TNFRF6/FAS, RRM2B, AQP3 and RPL3, 24 h after a 90 min or a 24 h-treatment with 5′-DFUR 250 μM. C_T values for each gene have been normalized to an endogenous reference gene (GAPDH). mRNA expression levels are given in arbitrary units using 24 h control as reference. Results are the mean ± S.E. of three experiments. Statistical significance was assessed using the Student's *t*-test ($^{*}P < 0.05$, $^{**}P < 0.01$, $^{***}P < 0.001$).

as targets of 5′-DFUR. The water channel aquaporin 3 (*AQP3*), which is a target for p73 [29], has no known relationship with 5′-DFUR or 5-FU, but it may be involved in cell volume increase associated with 5′-DFUR treatment (not shown). Down-regulation of two ribosomal proteins, *RPL3* and *RPL10*, was also detected and, interestingly, the effect was not blocked by NBTI. DNA-damaging agents induce stress responses that include repression of genes encoding ribosomal proteins [30]. Although such down-regulation due to 5-FU treatment has not yet been described, 5-FU misincorporation into RNA can result in toxicity at different levels [31]. Interestingly, p53 and genes implicated in growth arrest and apoptosis were induced after very short treatments (90 min) and the magnitude of these changes was similar to that obtained after a 24 h treatment. This observation clearly suggests that transcriptional activation of most drug targets do not indeed require long-term exposures.

However, the most striking result of our study came to light when analyzing the entry pathway of 5′-DFUR into MCF7 cells. 5′-DFUR has been shown to be taken up both by hENT1 and hENT2. In the present study, we have used a 5′-DFUR concentration close to the IC_{50} when hENT1 is inhibited (i.e., in the presence of NBTI) and, in these conditions, hENT2 is the main responsible for 5′-DFUR uptake. In spite of all this, however, NBTI blocked most of the transcriptional changes induced by 5′-DFUR, thus evidencing a key role of hENT1, but not hENT2, in a full cytotoxic response to this drug.

hENT1 abundance is highly variable in human tissues, and it seems to be over-expressed in some tumors, as deduced from labelled NBTI specific binding assays [32]. Furthermore, the cell content of hENT1 varies through the cell cycle [33], and high proliferation rates are associated with higher protein abundance of hENT1 [34]. Suitable antibodies against nucleoside transporters have recently been raised, thus allowing the analysis of a variety of tumors. hENT1 and hENT2 expression was retained in a high percentage (84–98%) of 300 gynecological tumors, while hCNT1 was lost in many cases (33–39%) [16]. Analysis of a cohort of 33 breast cancer patients showed at least four hENT1-deficient tumors and a high variability in hENT1 protein amounts [7]. Variability in hENT1 expression was also found in Reed-Sternberg cells of Hodgkin's disease [35].

Furthermore, clinical correlations between equilibrative nucleoside transporters and sensitivity to nucleoside analogs have been reported. hENT1 protein correlates with survival in a cohort of 21 patients suffering from pancreatic adenocarcinoma and treated with gemcitabine [10]. hENT1 expression correlates with *in vitro* resistance to ara-C in acute lymphoblastic leukaemia [36]. Moreover, acute myeloid patients who do not express hENT1-related mRNA have short disease-free survival after cytarabine treatment [37]. In mantle cell lymphoma, *ex vivo* sensitivity to gemcitabine correlates with hENT1 protein and hENT1-related mRNA expression [38]. Finally, in chronic lymphocytic leukaemia (CLL) *ex vivo* sensitivity to fludarabine correlates with hENT2 protein [9]. CLL is characterized by the accumulation of mature appearing B cells at G_0. However, all the studies in which hENT1 correlates with sensitivity were performed in highly proliferative tumors. Thus, the nucleoside transporter that modulates drug sensitivity might depend on the type of tumor and the nucleoside derivative used.

In summary, this study shows that most genes transcriptionally modified by the intermediate of capecitabine metabolism and immediate precursor of 5-FU, 5′-DFUR, are similar to those recently identified as 5-FU targets. Nevertheless, 5′-DFUR, but not 5-FU, is an hENT1 substrate, and so hENT1-mediated transport is also a good candidate to modulate nucleoside-derived drug cytotoxicity. This study demonstrates that hENT1 function is essential for the full transcriptional response to 5′-DFUR treatment, an observation that might help to understand the incipient clinical data suggesting a putative relationship between hENT1 expression and response to therapy and outcome.

Acknowledgments

Research grants: Supported by grants SAF2002-0717 and SAF2005-01259 (Ministerio de Educación y Ciencia, Spain) and Fundación Ramón Areces. MM-A holds a research fellowship from the Ministerio de Educación, Cultura y Deportes, Spain.

REFERENCES

[1] Longley DB, Harkin DP, Johnston PG. 5-Fluorouracil: mechanisms of action and clinical strategies. Nat Rev Cancer 2003;3:330–8.
[2] Baldwin SA, Beal PR, Yao SY, King AE, Cass CE, Young JD. The equilibrative nucleoside transporter family, SLC29. Pflugers Arch 2004;447:735–43.
[3] Gray JH, Owen RP, Giacomini KM. The concentrative nucleoside transporter family, SLC28. Pflugers Arch 2004;447:728–34.
[4] Pastor-Anglada M, Molina-Arcas M, Casado FJ, Bellosillo B, Colomer D, Gil J. Nucleoside transporters in chronic lymphocytic leukaemia. Leukemia 2004;18:385–93.
[5] Mata JF, Garcia-Manteiga JM, Lostao MP, Fernandez-Veledo S, Guillen-Gomez E, Larrayoz IM, et al. Role of the human concentrative nucleoside transporter (hCNT1) in the cytotoxic action of 5[Prime]-deoxy-5-fluorouridine, an active intermediate metabolite of capecitabine, a novel oral anticancer drug. Mol Pharmacol 2001;59:1542–8.
[6] Pastor-Anglada M, Casado FJ, Valdes R, Mata J, Garcia-Manteiga J, Molina M. Complex regulation of nucleoside transporter expression in epithelial and immune system cells. Mol Membr Biol 2001;18:81–5.
[7] Mackey JR, Jennings LL, Clarke ML, Santos CL, Dabbagh L, Vsianska M, et al. Immunohistochemical variation of human equilibrative nucleoside transporter 1 protein in primary breast cancers. Clin Cancer Res 2002;8:110–6.
[8] Molina-Arcas M, Bellosillo B, Casado FJ, Montserrat E, Gil J, Colomer D, et al. Fludarabine uptake mechanisms in B-cell chronic lymphocytic leukemia. Blood 2003;101:2328–34.
[9] Molina-Arcas M, Marce S, Villamor N, Huber-Ruano I, Casado FJ, Bellosillo B, et al. Equilibrative nucleoside transporter-2 (hENT2) protein expression correlates with ex vivo sensitivity to fludarabine in chronic lymphocytic leukemia (CLL) cells. Leukemia 2005;19:64–8.
[10] Spratlin J, Sangha R, Glubrecht D, Dabbagh L, Young JD, Dumontet C, et al. The absence of human equilibrative nucleoside transporter 1 is associated with reduced survival in patients with gemcitabine-treated pancreas adenocarcinoma. Clin Cancer Res 2004;10:6956–61.
[11] Fernandez-Veledo S, Valdes R, Wallenius V, Casado FJ, Pastor-Anglada M. Up-regulation of the high-affinity pyrimidine-preferring nucleoside transporter concentrative nucleoside transporter 1 by tumor necrosis factor-alpha and interleukin-6 in liver parenchymal cells. J Hepatol 2004;41:538–44.
[12] Tracey L, Villuendas R, Ortiz P, Dopazo A, Spiteri I, Lombardia L, et al. Identification of genes involved in resistance to interferon-alpha in cutaneous T-cell lymphoma. Am J Pathol 2002;161:1825–37.
[13] Vaquerizas JM, Dopazo J, Diaz-Uriarte R. DNMAD: web-based diagnosis and normalization for microarray data. Bioinformatics 2004;20:3656–8.
[14] Herrero J, Diaz-Uriarte R, Dopazo J. Gene expression data preprocessing. Bioinformatics 2003;19:655–6.
[15] Cheng Y, Prusoff WH. Relationship between the inhibition constant (K1) and the concentration of inhibitor which causes 50 percent inhibition (I50) of an enzymatic reaction. Biochem Pharmacol 1973;22:3099–108.
[16] Farre X, Guillen-Gomez E, Sanchez L, Hardisson D, Plaza Y, Lloberas J, et al. Expression of the nucleoside-derived drug transporters hCNT1, hENT1 and hENT2 in gynecologic tumors. Int J Cancer 2004;112:959–66.
[17] Mackey JR, Mani RS, Selner M, Mowles D, Young JD, Belt JA, et al. Functional nucleoside transporters are required for gemcitabine influx and manifestation of toxicity in cancer cell lines. Cancer Res 1998;58:4349–57.
[18] Gati WP, Paterson AR, Belch AR, Chlumecky V, Larratt LM, Mant MJ, et al. Es nucleoside transporter content of acute leukemia cells: role in cell sensitivity to cytarabine (araC). Leuk Lymphoma 1998;32:45–54.
[19] Backus HH, Pinedo HM, Wouters D, Kuiper CM, Jansen G, van Groeningen CJ, et al. Differences in the induction of

DNA damage, cell cycle arrest, and cell death by 5-fluorouracil and antifolates. Oncol Res 2000;12:231–9.
[20] Troester MA, Hoadley KA, Sorlie T, Herbert BS, Borresen-Dale AL, Lonning PE, et al. Cell-type-specific responses to chemotherapeutics in breast cancer. Cancer Res 2004;64:4218–26.
[21] Park JS, Young Yoon S, Kim JM, Yeom YI, Kim YS, Kim NS. Identification of novel genes associated with the response to 5-FU treatment in gastric cancer cell lines using a cDNA microarray. Cancer Lett 2004;214:19–33.
[22] Reigner B, Watanabe T, Schuller J, Lucraft H, Sasaki Y, Bridgewater J, et al. Pharmacokinetics of capecitabine (Xeloda) in Japanese and Caucasian patients with breast cancer. Cancer Chemother Pharmacol 2003;52:193–201.
[23] Rosenwald A, Chuang EY, Davis RE, Wiestner A, Alizadeh AA, Arthur DC, et al. Fludarabine treatment of patients with chronic lymphocytic leukemia induces a p53-dependent gene expression response. Blood 2004;104:1428–34.
[24] Liu G, Chen X. The ferredoxin reductase gene is regulated by the p53 family and sensitizes cells to oxidative stress-induced apoptosis. Oncogene 2002;21:7195–204.
[25] Okamura S, Arakawa H, Tanaka T, Nakanishi H, Ng CC, Taya Y, et al. p53DINP1, a p53-inducible gene, regulates p53-dependent apoptosis. Mol Cell 2001;8:85–94.
[26] Zhao R, Gish K, Murphy M, Yin Y, Notterman D, Hoffman WH, et al. Analysis of p53-regulated gene expression patterns using oligonucleotide arrays. Genes Dev 2000;14:981–93.
[27] Kho PS, Wang Z, Zhuang L, Li Y, Chew JL, Ng HH, et al. p53-regulated transcriptional program associated with genotoxic stress-induced apoptosis. J Biol Chem 2004;279:21183–92.
[28] Hernandez-Vargas H, Ballestar E, Carmona-Saez P, von Kobbe C, Banon-Rodriguez I, Esteller M, et al. Transcriptional profiling of MCF7 breast cancer cells in response to 5-fluorouracil: relationship with cell cycle changes and apoptosis, and identification of novel targets of p53. Int J Cancer 2006;119:1164–75.
[29] Zheng X, Chen X. Aquaporin 3, a glycerol and water transporter, is regulated by p73 of the p53 family. FEBS Lett 2001;489:4–7.
[30] Gasch AP, Spellman PT, Kao CM, Carmel-Harel O, Eisen MB, Storz G, et al. Genomic expression programs in the response of yeast cells to environmental changes. Mol Biol Cell 2000;11:4241–57.
[31] Kanamaru R, Kakuta H, Sato T, Ishioka C, Wakui A. The inhibitory effects of 5-fluorouracil on the metabolism of preribosomal and ribosomal RNA in L-1210 cells in vitro. Cancer Chemother Pharmacol 1986;17:43–6.
[32] Goh LB, Mack P, Lee CW. Nitrobenzylthioinosine-binding protein overexpression in human breast, liver, stomach and colorectal tumour tissues. Anticancer Res 1995;15:2575–9.
[33] Pressacco J, Wiley JS, Jamieson GP, Erlichman C, Hedley DW. Modulation of the equilibrative nucleoside transporter by inhibitors of DNA synthesis. Br J Cancer 1995;72:939–42.
[34] Wiley JS, Cebon JS, Jamieson GP, Szer J, Gibson J, Woodruff RK, et al. Assessment of proliferative responses to granulocyte-macrophage colony-stimulating factor (GM-CSF) in acute myeloid leukaemia using a fluorescent ligand for the nucleoside transporter. Leukemia 1994;8: 181–5.
[35] Reiman T, Clarke ML, Dabbagh L, Vsianska M, Coupland RW, Belch AR, et al. Differential expression of human equilibrative nucleoside transporter 1 (hENT1) protein in the Reed-Sternberg cells of Hodgkin's disease. Leuk Lymphoma 2002;43:1435–40.
[36] Stam RW, den Boer ML, Meijerink JP, Ebus ME, Peters GJ, Noordhuis P, et al. Differential mRNA expression of Ara-C-metabolizing enzymes explains Ara-C sensitivity in MLL gene-rearranged infant acute lymphoblastic leukemia. Blood 2003;101:1270–6.
[37] Galmarini CM, Thomas X, Calvo F, Rousselot P, Rabilloud M, El Jaffari A, et al. In vivo mechanisms of resistance to cytarabine in acute myeloid leukaemia. Br J Haematol 2002;117:860–8.
[38] Marce S, Molina-Arcas M, Villamor N, Casado FJ, Campo E, Pastor-Anglada M, et al. Expression of human equilibrative nucleoside transporter 1 (hENT1) and its correlation with gemcitabine uptake and cytotoxicity in mantle cell lymphoma. Haematologica 2006;91:895–902.